Simulation of ITER Transient Heat Loads to the Divertor Surfaces with Using the High Power Quasi-Steady-State Plasma Accelerator

V. I. Tereshin 1), A. N. Bandura 1), O. V. Byrka 1), V. V. Chebotarev 1), I. E. Garkusha 1), I. Landman 2), V. A. Makhlaj 1), D. G. Solyakov 1)

1) Institute of Plasma Physics of the NSC KIPT, Kharkov, 61108, Ukraine
2) Forschungszentrum Karlsruhe, IHM, 76021 Karlsruhe, Germany

e-mail: tereshin@ipp.kharkov.ua

Abstract. The behavior of the surfaces of materials, relevant for ITER divertor plates, was investigated under the heat loads of wide range (0.5 – 30 MJ/m^2) typical for conditions of current disruptions and ELMs in tokamak-reactor. The experiments were carried out with using the powerful plasma streams generated by quasi-steady-state plasma accelerator QSPA Kh-50, which characterized by essentially longer duration (~ 0.25 ms) of plasma stream generation in comparison with pulsed plasma guns. The main emphasis was placed on repetitive loading, typical for ELMs in ITER, when exposing the tungsten, graphite and different combined W-C targets. Onset of vapor shield formation in front of the surface under ELM-like plasma loads was studied. Achievement of evaporation threshold for exposed targets resulted in almost saturation of the surface heat load with further increase of the plasma energy density. For tungsten targets the vapor shield and its influence on plasma energy transfer to the surface become clearly seen when the surface heat load achieved 1.1 MJ/m^2. It was shown that the repetitive heat loads (up to 450 cycles) led to the formation of two types of cracks at the tungsten surface: macro cracks (with mesh size of an order 1 mm) and the net of intergrannular micro cracks (with the mesh of 10-20 μm). They have principally different physical nature. High-speed imaging showed non-uniform surface heating and formation of overheated areas (hot spots of ~ (0.1 - 0.5) mm were formed at the surface) even for exposures of isotropic fine grain graphite MPG-7. Plasma impacts caused the droplets splashing from the tungsten surface. Angular distribution of splashed droplets was analyzed. Droplets continued to be ejected from the melt after plasma impact during > 10 ms. Droplets velocities could achieve several tens m/s.

1. Introduction

Experimental investigations of plasma-surface interaction (PSI) in conditions simulating transient events in fusion reactor ITER are of importance for the determination of erosion mechanisms of plasma facing materials, dynamics of erosion products, the impurities transport in the plasma, the vapor shield effects and its influence on plasma energy transfer to the material surface. In turn, the obtained results are used for validation of predictive models developed for ITER and DEMO, estimation of tolerable size of Type I ELMs and lifetime of divertor armour materials.

As it was shown earlier in disruption simulation experiments with plasma guns [1,2] and in numerical modeling [3,4] the main feature of high-power plasma interaction with material surfaces is formation of dense plasma shield in front of the target surface. For disruption-like loads of ~ (10-20) MJ/m^2 only several percents of the plasma energy reached the surface due to the strong shielding effect [1,2]. It should be mentioned that dense vapor shield formation in disruption simulation experiments was studied mainly for graphite and CFC targets. For the ELMs, and their impact to the tungsten surface, the shielding layer properties have yet to be investigated especially for the plasma loads, which are close to the evaporation threshold.

Energy densities deposited during ELMs are much less than disruption ones. The ELM heat loads in ITER are expected to be Q < 3 MJ/m^2 during τ = (0.1 - 0.5) ms [5]. However, some shielding effects can also appear in this case. Onset of vapor shield and effects of “weak” shielding for a single ELM may contribute significantly to the resulting surface damage due to expected large number (up to 10^6) of repetitive ELMs.

First stage of the ITER operation is foreseen with using both tungsten and CFC as adjoin materials for divertor components which are able to withstand the transient high heat loads [5]. Therefore PSI issues resulting from mutual neighborhood of tungsten and carbon on the divertor plate surfaces should be analyzed comprehensively. This is important from the point of view of redeposition issues and chemical reactions (carbides etc.) and also for analysis of erosion characteristics of combined targets with adjoined W and C areas and features of plasma-surface interaction under the transient events, like ELMs.
This paper presents the results of experiments on high power plasma interaction with material surfaces under conditions typical for ITER Type I ELMs including the measurements of plasma energy transfer to the material surface as a function of the impact load and onset of vapor shield for W, C and adjoined W-C surfaces under repetitive ELM relevant plasma exposures.

2. Experimental Setup

The samples have been exposed to hydrogen plasma streams produced by the quasi-steady-state plasma accelerator QSPA Kh-50, described elsewhere [6-8]. Scheme of plasma exposures is presented in Fig. 1. QSPA Kh-50 consists of two stages. The first one is used for plasma production and pre-acceleration. The main second stage is a coaxial system of shaped active electrodes with magnetically screened elements, supplied from independent power sources. The plasma streams, generated by QSPA Kh-50, are injected into the magnetic system of 1.6 m in length and 0.44 m in inner diameter with a magnetic field of up to 0.54 T in diagnostic chamber where the targets have been installed (Fig. 1).
The experiments were performed with repetitive pulses of the duration of 0.25 ms and the heat loads in the range of (0.2 – 2.5) MJ/m^2, which simulate the ELMs impact in ITER. The plasma stream diameter is 18 cm, the ion energy is about 0.4 keV, and maximum plasma pressure achieves 3.2 bar. Plasma heat loads were varied by both changing the scenario of gas filling to the accelerator channel and changing the working voltage at the accelerator electrodes.
Most of targets were exposed to perpendicular plasma irradiation with various number of pulses. Some experiments were carried out with targets preliminary heated above the DBTT temperature to decrease the brittleness. In this case Ohmic heater was installed at the back side of the target. It provides the target heating in vacuum conditions (to avoid oxidation) prior to the exposure and the target temperature was kept at the level of 650 C^0 for each plasma pulse.

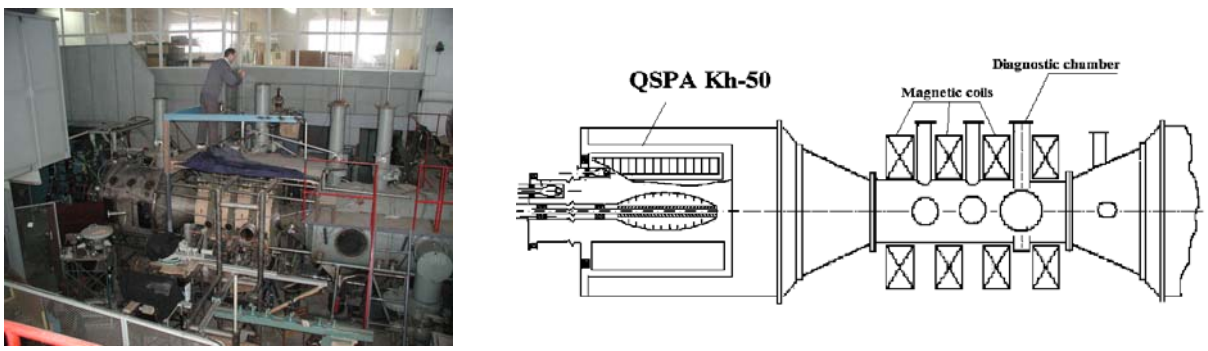

Fig. 1. General view and scheme of experimental device (scheme of targets exposures).

Calorimetry (both at plasma stream and at the target surfaces), piezo-detectors, electric and magnetic probes, interferometry, spectroscopy and other diagnostics were applied for measurements of plasma stream parameters and surface heat loads in different regimes of operation. Observations of plasma interactions with exposed surfaces and droplets monitoring were performed with high-speed CMOS camera PCO AG**.** X-ray diffraction measurements, optical and SEM microscopy and so on were used for surface analysis.

3. Experimental Results

Fig.2. shows the heat load to the tungsten, graphite and combined W-C target surfaces, which was measured with calorimetry, in dependence on energy density of impacting plasma stream. For tungsten target exposure the onset of melting is observed on the surface at the surface heat load of 0.57 MJ/m^2. The measurements demonstrate that even for plasma exposures, which not result in the melting, the absorbed heat load is about 55-60 % of the impact plasma energy. The dynamical screening of the surface from impacting plasma stream appears in this case probably due to the shock wave formation and plasma stream thermalization under the interaction with the target surface. The stopped plasma layer, formed from the head of the plasma stream, ceases to be completely transparent for subsequently impacting plasma ions. Tungsten vapor shield formation and its influence on plasma energy transfer to the surface becomes clearly seen as the surface heat load achieves 1.1 MJ/m^2. The fraction of plasma energy, which is absorbed by the target surface, is rapidly decreased with achieving the evaporation onset for exposed targets. At this, the value of heat load to the surface remains practically constant with further increase of the energy density of impacting plasma (plateau region in Fig. 2).

The evaporation leads to enhanced mass losses of tungsten: increase of the heat load from 0.75 to 1.1 MJ/m^2 raises mass losses for one order of magnitude and causes bubble structures at the surface. Due to achievement of evaporation threshold the erosion crater become visible even on the “background” of the surface roughness and swelling. The erosion rate, caused by evaporation, is ~ 0.05 μm/pulse. Microscopy observations of tungsten targets show boiling bubbles on the surface exposed with heat load of 1.1 MJ/m^2 (Fig. 3). For initial pulses the boiling is initiated on the surface by impurities. With further exposures it becomes predominantly volumetric and deep bubbles are arisen at the surface. The volumetric boiling occurs predominantly at the vicinity of crack edges.

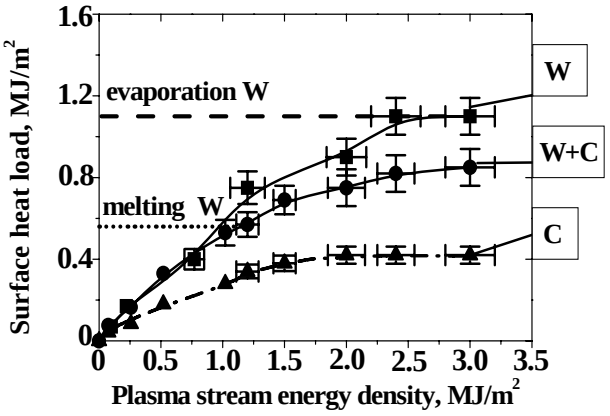

Fig.2. Heat load to the target surfaces vs. the energy density of impacting plasma stream.

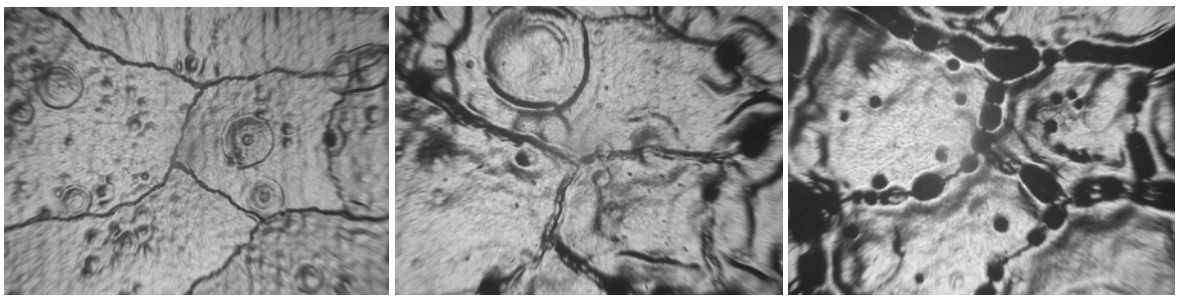

Fig.3. Boiling bubbles on the tungsten surface, exposed with 5, 25 and 80 pulses of 1.1 MJ/m^2 (the same surface region).

It was shown that the repetitive heat loads (up to 450 cycles), typical for ELMs in ITER, lead to the formation of two types cracks at the tungsten surface: macro cracks (with mesh size of an order 1 mm) and the net of intergrannular micro cracks (with the mesh of 10-20 μm).
Evolution of macro cracks in the course of plasma exposures is shown in Fig. 4. Crack width is increased with pulse number with following saturation after about 200 pulses. Nevertheless the crack width achieves several tens microns in result of plasma exposures demonstrating significant damage of tungsten surface.
It is shown that macro and micro cracks have principally different physical nature. Macro cracks are the result of transition from ductile to brittle state at the process of the surface layer cooling (i.e. ductile to brittle transition). At the same time the fine cracks are the attribute of intensive melting and their formation is dealing with non-equilibrium solidification of melt. This is confirmed by the fact that under the irradiation of preliminary heated target up to the temperature of 650 ^{0}C (above the temperature of ductile to brittle transition) the macro cracks are not observed while the micro cracks are developed on the surface, similarly to non heated targets.
Measurements of the energy transfer to combined tungsten-graphite targets of different sizes demonstrate that the value of energy density delivered to such target surface is reduced in comparison with the irradiation of the pure tungsten target (Fig. 2). Carbon neighborhood resulted in the shielding which has been developed for lower heat loads. Experiments with

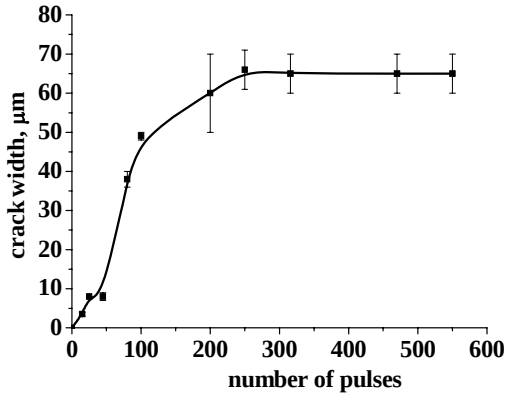

Fig.4. Evolution of macro cracks on the tungsten surface, exposed with repetitive pulses of 0.75 MJ/m^2.

MPG-7 graphite targets show that carbon evaporation starts at (0.4 - 0.45) MJ/m^2. Carbon vapor shield formation during exposures of combined W-C targets results in additional decrease of the heat loads to W surface (from 1.1 MJ/m^2 to (0.8 – 85) MJ/m^2) preventing tungsten evaporation. It should be noted that tungsten evaporation threshold in the case of adjoined graphite surface was not achieved even with increasing plasma stream energy density (Fig. 2).

Plasma impacts with the loads above the melting threshold cause the droplets splashing from the tungsten surface. As an example, Fig 5 shows images of the droplets traces for different time moments after the end of the plasma pulse. The applied measurement scheme for droplets monitoring was similar to used in [9, 10]. Exposition time for each image is 1.2 ms and the velocity of the droplets can be estimated from the lengths of their traces. Movement in perpendicular direction to the image plane is derived from consecutive frames. Consequences of the images form movie with possibility to analyze the dynamics of droplets splashing from the surface.

Droplets continue to be ejected from the melt after plasma impact during > 10 ms. It is obtained that droplets velocities may achieve several tens m/s. Fast droplets were generated at earlier time moments. Smaller velocities are observed for late stage of observation (Fig. 5). During intermediate stage both groups of droplets with fast and lower velocities have been observed (Figs. 5 and 6a).

Angular distribution of ejected droplets is presented in Fig. 6b. For perpendicular to the surface plasma impacts droplets are ejected primarily with small angles to the normal. Nevertheless rather large angles up to 80^0 are measured also. Analysis of droplet traces from consecutive images show the influence of gravitational force for droplets with higher mass

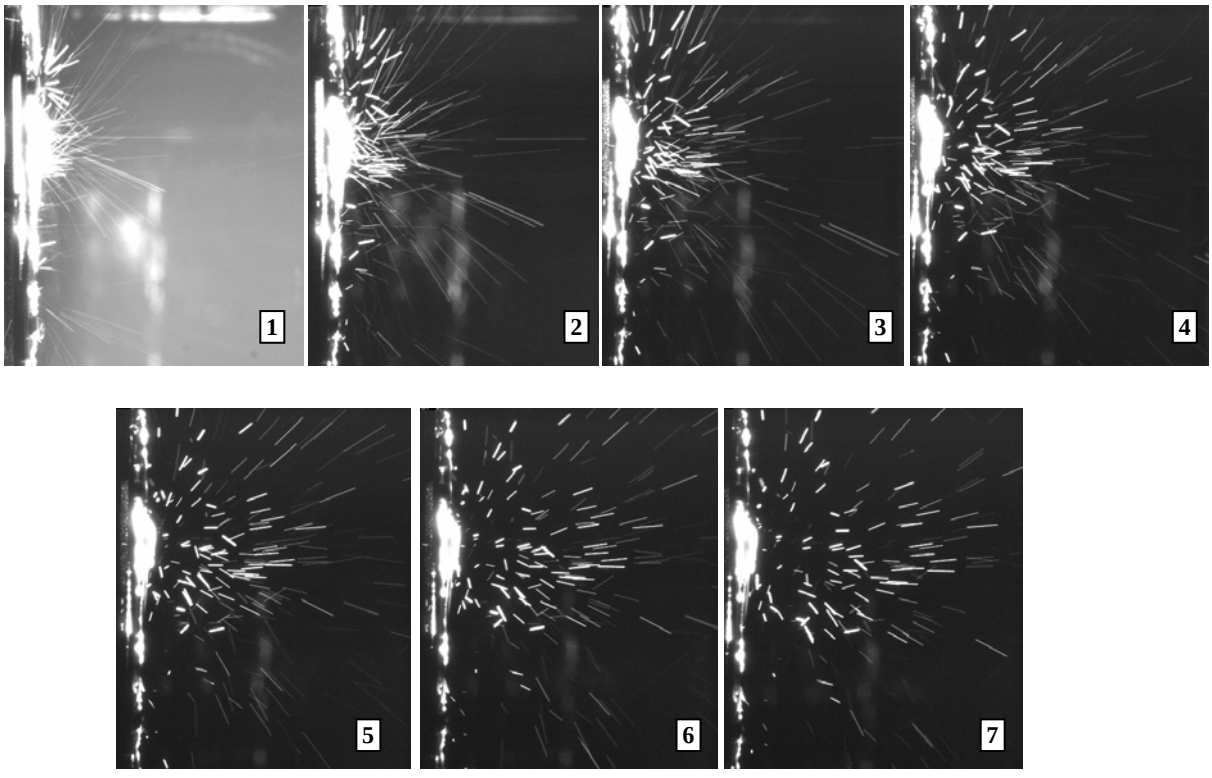

Fig.5. Droplets splashing from tungsten melt. Images of droplet traces: t_1 = 1.8 ms, t_2 = 3.0 ms, t_3 = 4.2 ms, t_4 = 5.4 ms, t_5 = 6.6 ms, t_6 = 7.8 ms, t_7 = 9.0 ms after the end of plasma pulse, ($t_{exposure}$ = 1.2 ms).

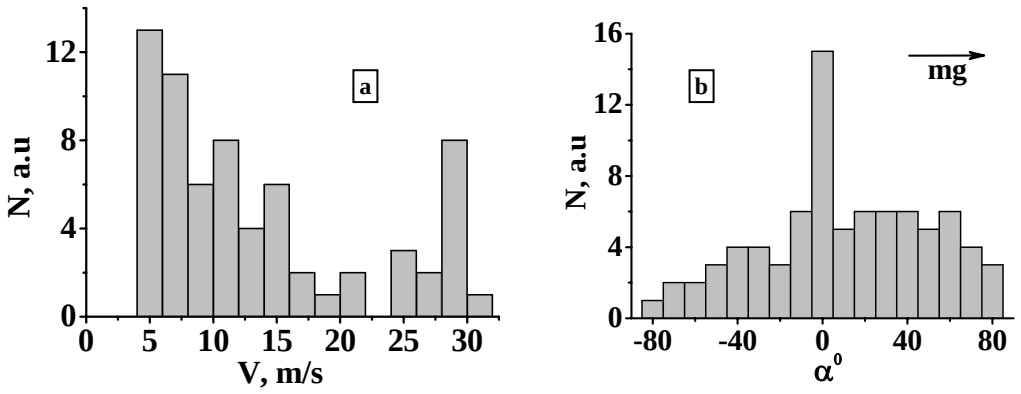

Fig.6. Velocity (a) and angular (b) distributions of ejected droplets.

and smaller velocities. Due to the gravitation the resulting angular distribution of the droplets became non-symmetric (Fig.6b). With achieving evaporation threshold the tungsten boiling results in intensification of the droplets splashing. Their size is varied in the range of (5-100) μm.

Dynamics of tungsten and carbon vapor in front of the targets surfaces, which was studied with spectroscopy and high-speed photography during the plasma pulse, and it dependence on the magnitude of external magnetic field is described in [8]. Here it can be only mentioned that evaporated tungsten is concentrated in rather thin plasma layer of < 0.5 cm close to the surface and it does not propagate significantly in upstream direction during the QSPA pulse. In the case of graphite target exposure, high-speed photography shows continuous region of carbon vapor luminosity. Thickness of the shielding layer increases during the pulse and exceeds 5 cm. Spectroscopy measurements demonstrate that carbon lines are registered not only in front of the target surface, but also for larger distances (up to 20 cm) from the target.

Fig.7 shows the hot spots indicating overheated local areas on the graphite surface of combined W-C target (tungsten rod of 1 cm diameter surrounded by MPG-7 graphite of 8 cm in diameter). The target was subjected to inclined plasma impact, $\alpha = 45^0$. Surface heat load

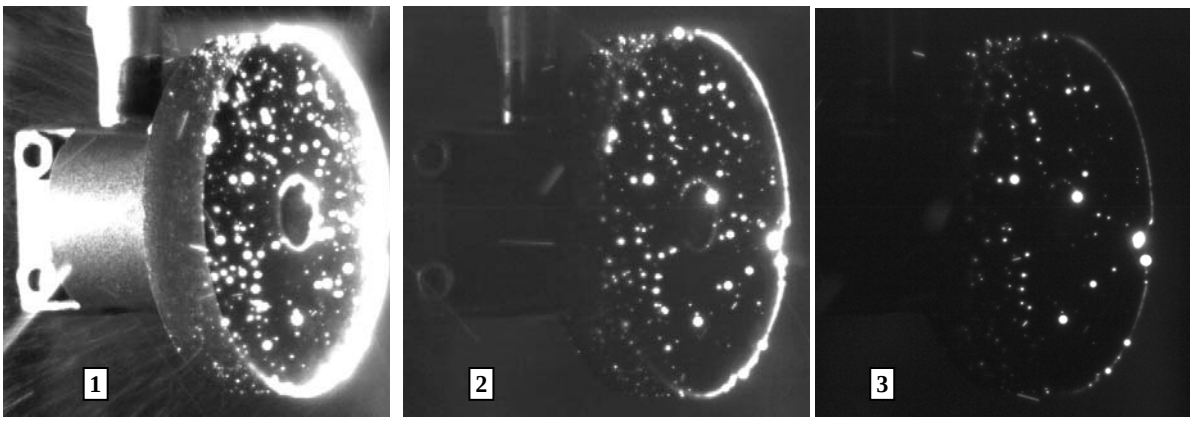

Fig.7. Images of hot spots on graphite surface of combined W-C target (W rod of 1 cm in diameter surrounded by MPG-7 graphite of 8 cm in diameter) indicating overheated areas (1-3). Inclined impact $\alpha = 45^0$, $t_{exp} = 0.5$ ms, $t_1 = 0.7$ ms, $t_2 = 1.7$ ms, $t_3 = 3.7$ ms after pulse, $Q_{surf} = 0.5$ MJ/m^2.

Q_{surf} = 0.5 MJ/m^2. The images correspond to t_{start} = 0.7 ms and t_{start} = 3.7 ms after plasma pulse respectively. Exposition time of each image is t_{exp} = 0.5 ms. It should be noted much more pronounced heating of upstream part of the inclined target edge, which is demonstrated by Fig.7. This is valid also for tungsten rod in target center (Fig.7.1).
The hot spots are probably formed on graphite surface due to the surface relief developed. The heat load to the inclined target surface (0.5 MJ/m^2) is below the melting threshold of tungsten. Thus the observed bright spots are not caused by W droplets. Corresponding high-speed imaging had proved that this luminosity can not also be attributed to carbon dust, which could be redeposited back to the surface in the end on plasma pulse. The hot spots indicate the areas of enhanced evaporation and their luminosity is observed during ~ 30 ms after plasma impact. Size distributions of the hot spots are also presented in Fig.8 for time moments of t_1 and t_3. It was impossible to perform analysis of micro-spots with larger magnification while the target is in vacuum chamber. Nevertheless, most of registered spots are of ~ (0.1 - 0.5) mm in diameter, which is much larger than maximal size of the grains in MPG-7 graphite ((10 - 25) μm). Qualitatively the size distribution of the spots remains similar for different time moments after the end of pulse. The only number of overheated areas is decreased and luminosity of some spots disappears with time.

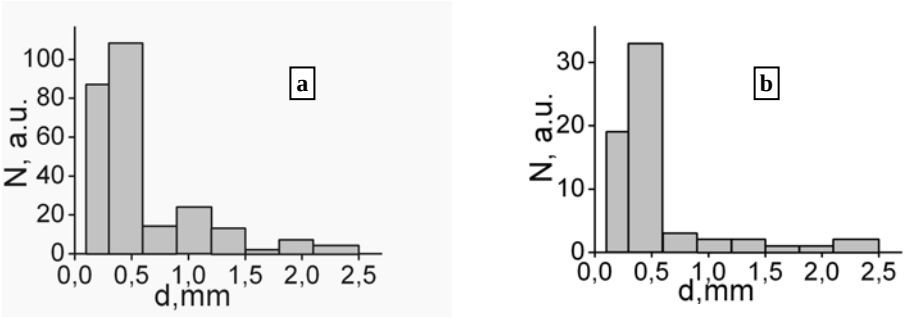

Fig.8. Size distributions of hot spots at the moments of t_1 (a) and t_3 (b).

4. Conclusions

Features of plasma-surface interaction and plasma energy transfer to the material surface are studied in dependence on plasma heat loads in ELM simulation experiments with QSPA Kh-50. Plasma exposures of tungsten, graphite and different combined W-C targets were performed with repetitive pulses of 0.25 ms in duration and the heat loads varied in the range of (0.2-2.5) MJ/m^2.
Onset of vapor shield formation in front of the surface under ELM-like plasma loads was studied. Achievement of evaporation threshold for exposed targets resulted in almost saturation of the surface heat load with further increase of the plasma energy density. For tungsten targets the vapor shield and its influence on plasma energy transfer to the surface become clearly seen when the surface heat load achieved 1.1 MJ/m^2. The evaporation resulted in enhanced mass losses of tungsten, formation of erosion crater and bubbles on the surface.
Influence of carbon PFCs neighborhood on the plasma energy transfer to the tungsten surface was demonstrated. Carbon neighborhood resulted in protection of tungsten surface starting with lower heat loads. Carbon become to evaporate at (0.4 - 0.45) MJ/m^2 and its vapor shield formation resulted in additional decrease of heat loads to the tungsten surface (from 1.1 MJ/m^2 to (0.8 - 0.85) MJ/m^2) preventing tungsten evaporation.

High-speed imaging showed non-uniform surface heating and formation of overheated areas even for exposures of isotropic fine grain graphite MPG-7. Hot spots of ~ (0.1 - 0.5) mm were formed on graphite surface probably due to the surface relief developed. Hot spots indicated the areas of enhanced evaporation and their luminosity was observed during ~ 30 ms after plasma impact.
Plasma impacts caused the droplets splashing from the tungsten surface. Angular distribution of splashed droplets was analyzed. Droplets continued to be ejected from the melt after plasma impact during ~ 10 ms. Droplets velocities could achieve several tens m/s. Fast droplets were generated at earlier time moments. Smaller velocities corresponded to late stage of observation.

Acknowledgements

This work has been supported in part by STCU project #4155. The authors would like to acknowledge N.V. Kulik, V.V. Staltsov, S.I. Lebedev and P.V. Shevchuk for assisting in the experiments.

References

[1] CHEBOTAREV, V.V., et al., "Characteristics of the transient plasma layers produced by irradiation of graphite targets by high power quasi-stationary plasma streams under the disruption modeling experiments", J. Nucl. Mater. **233-237** (1996) 736.
[2] ARKHIPOV, N., et al. " Plasma /surface interaction in ITER tokamak disruption simulation experiments", Fusion Technology **32** (1997) 45.
[3] WÜRZ, H., et al., "Experimental simulation and numerical modeling of vapor shield formation and divertor material erosion for ITER typical plasma disruption", J. Nucl. Mater. **220-222** (1995) 1066.
[4] HASSANEIN, A., KONKASHBAEV, I., "Lifetime evaluation of plasma-facing materials during a tokamak disruption", J. Nucl. Mater. **233-237** (1996) 713.
[5] FEDERICI, G., et al., "Assessment of erosion of the ITER divertor targets during type I ELMs", Plasma Phys. Control. Fus., **45** (2003) 1523.
[6] GARKUSHA, I.E., et al., "Tungsten melt layer erosion due to $\vec{J} \times \vec{B}$ force under conditions relevant to ITER ELMs", J. Nucl. Mater. **363-365** (2007) 1021.
[7] MAKHLAJ, V.A., et al., **"**Effect of preheating on the damage to tungsten targets after repetitive ITER ELM-like Heat Loads", Physica Scripta **T128** (2007) 111.
[8] TERESHIN, V.I., et al., "Application of powerful quasi-steady-state plasma accelerators for simulation of ITER transient heat loads on divertor surfaces", Plasma Phys. Control. Fus. **49** (2007) A231.
[9] ZHITLUKHIN, A., et al., "Effect of ELMs and disruptions on ITER divertor armor materials", J. Nucl. Mater. **363-365** (2007) 301.
[10] LINKE, J., et al., "Carbon Particles Emission, Brittle Destruction and Co-deposit Formation: Experience from Electron Beam Experiments and Controlled Fusion Devices", Physica Scripta. **T91** (2001) 36.